MATHEMATICAL SIMULATION OF THE FORMATION OF SMALL HOLES DURING ELECTROCHEMICAL MACHINING

Petr NOVÁK[a], Ivo ROUŠAR[a], Arnošt KIMLA[b], Vladimír MEJTA[a] and Václav CEZNER[a]

[a] *Department of Inorganic Technology and*
[b] *Department of Mathematics,*
Prague Institute of Chemical Technology, 166 28 Prague 6

Received September 12th, 1980

For the purpose of studying the formation of small holes during electrochemical machining, a two-fold transformation of the interelectrode space to a rectangle was used (threedimensional system symmetrical around the axis of the hole) and a superrelaxation method for the calculation of the potentials in this region was proposed. The results for the case of primary current distribution are compared with those involving polarization of the electrodes, heating of the streaming electrolyte by the Joule heat, and the formation of the gas phase. It is shown that the primary current distribution represents a sufficient approximation of the situation during machining.

In proposing tools for electrochemical machining, either approximate methods are used[1-3] or a solution of the Laplace equation for the given interelectrode space[4-6]. Owing to difficulties involved in solving such problems, electrodes without polarization are usually considered. The present work deals with calculations for a real case of electrochemical drilling, showing changes in the form of the workpiece caused by heating of the electrolyte, bubble formation, and polarization of the electrodes during machining.

FORMULATION OF THE PROBLEM

The shape of the cathode does not change during electrochemical machining, whereas the anode dissolves gradually by the action of direct current, and its shape changes accordingly. We shall consider the three-dimensional case, where the anode is initially plane and the cathode is a hollow cylinder whose outer surface is insulated. The electrolyte streams through the hollow cathode against the anode, as shown in Fig. 1.

The process of drilling a hole in the anode can be simulated by the following sequence of calculations: *1*) We calculate the distribution of potentials in the space delimited by the cathode and anode. *2*) We calculate the local current densities on both electrodes. *3*) We choose a time interval, $\Delta\tau$, and calculate the loss of metal due to electrochemical dissolution of the anode in a given place from Faraday's law. In the case of anodic evolution of oxygen we take the corresponding current loss into

account. We calculate the changes of the coordinates of the points on the curve γ $(x', y', z') = 0$, expressing the shape of the anode, in the direction of the normal. We assume that the cathode moves at constant velocity, v_x, toward the anode. Thus, we find the curve describing the new shape of the anode surface. The real course of the machining will be naturally described by this simulation the better the smaller will be the value of $\Delta\tau$. *4)* The new shape of the anode will be approximated by a finite set of points (x'_i, y'_i, z'_i), $i = 1, 2, \ldots, N$. *5)* We return to point *1)*; if the shape of the anode surface in the given region does not change any more within the limits of the desired accuracy, a stationary state is attained and the calculation is stopped.

With the use of the finite difference method with fixed grid points, it would be necessary to consider the location of the grid points on the boundary and to calculate their distances from the neighbouring grid points. Since this method of calculation of the potentials on the anode surface and the programming would be very difficult, it is preferable to use more complicated relations for the calculation of potentials in the interelectrode space and to preserve the form of the boundary conditions for the calculation of the potentials regardless of the changing form of the anode. This is possible if the interelectrode space is transformed to a rectangle.

Transformation of the Interelectrode Space to a Rectangle

Since the system is symmetrical with respect to the x' axis (Fig. 1), it is preferable to use spherical coordinates. All properties of the system are functions of the angle ω

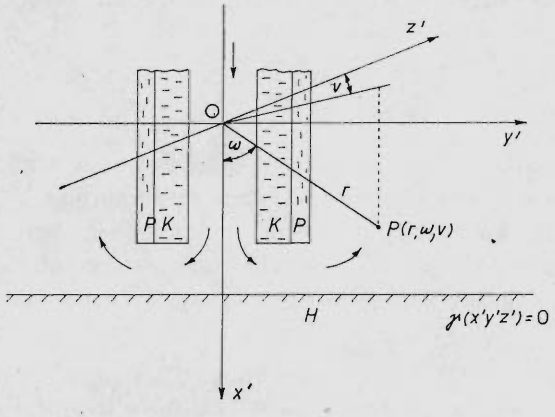

FIG. 1

Cross section of model system with cartesian and spherical coordinates. *K* metal capillary (cathode); *P* insulating layer; *H* workpiece (anode); arrows denote electrolyte flow

and radius r only. We introduce new two-dimensional cartesian coordinates x, y in an arbitrary section passing through the x' axis so that

$$x = x' , \quad y = (y'^2 + z'^2)^{1/2} . \qquad (1), (2)$$

The coordinates r, ω can then be interpreted as polar coordinates in the x, y plane. The mathematical description of the system in the coordinates r, ω and x, y will be used with advantage in further calculations.

In the space between the electrodes we have

$$\operatorname{div} i = 0 , \quad i = (1/\varrho_M) \operatorname{grad} \varphi , \qquad (3), (4)$$

whence we obtain the starting partial differential equation, which is to be solved:

$$\frac{\partial^2 \varphi}{\partial r^2} + \frac{1}{r^2} \frac{\partial^2 \varphi}{\partial \omega^2} + \left(\frac{2}{r} - \frac{1}{\varrho_M} \frac{\partial \varrho_M}{\partial r} \right) \frac{\partial \varphi}{\partial r} + \frac{1}{r^2} \left(\frac{1}{\operatorname{tg} \omega} - \frac{1}{\varrho_M} \frac{\partial \varrho_M}{\partial \omega} \right) \frac{\partial \varphi}{\partial \omega} = 0 . \qquad (5)$$

We shall divide the interelectrode space into parts *1* and *2* (Fig. 2). The limits of the system after transformation to polar coordinates are shown in Fig. 3. In this trans-

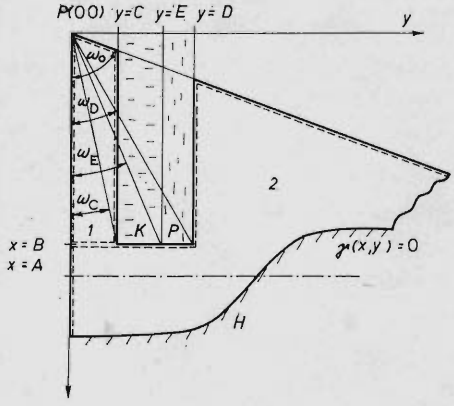

FIG. 2

Cross section through the system; the interelectrode space is divided by dashed lines into parts *1* and *2*. *A*, *B*, *C*, *D*, *E* longitudinal dimensions; $\gamma(x, y)$ contour of anode; x, y coordinates; *K*, *P*, *H* see Fig. 1

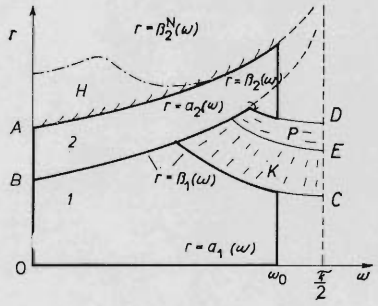

FIG. 3

Interelectrode space transformed to polar coordinates r, ω

formation, the origin of coordinates, $r = 0$, plays the role of a singular point and is transformed to a straight line representing the axis ω and forming a part of the limits of the system with equation $\alpha_1(\omega) = 0$. Since this refers to a single point, the potential on this limit is independent of ω. Other equations of the limits of the system are as follows:

$$\beta_1(\omega) = \begin{cases} \mathrm{B}/\cos\omega\colon \omega \in \langle 0, \omega_\mathrm{C}\rangle \\ \mathrm{C}/\sin\omega\colon \omega \in \langle \omega_\mathrm{C}, \omega_0\rangle \end{cases} \tag{6}$$

$$\alpha_2(\omega) = \begin{cases} \mathrm{B}/\cos\omega\colon \omega \in \langle 0, \omega_\mathrm{D}\rangle \\ \mathrm{D}/\sin\omega\colon \omega \in \langle \omega_\mathrm{D}, \omega_0\rangle \end{cases} \tag{7}$$

$$\beta_2(\omega) = \mathrm{A}/\cos\omega\,. \tag{8}$$

The boundary conditions are:

$$\partial\varphi/\partial r = 0 \quad \text{for} \quad r = 0 \tag{9}$$

$$\partial\varphi/\partial\omega = 0 \quad \text{for} \quad \omega = 0,\ \omega = \omega_0 \tag{10}$$

$$\varphi = \varphi(i_\mathrm{N}) \quad \text{for} \quad r = \beta_1(\omega),\ \omega \in \langle \omega_\mathrm{C}, \omega_0\rangle$$
$$r = \alpha_2(\omega),\ \omega \in \langle \omega_\mathrm{C}, \omega_\mathrm{E}\rangle$$
$$r = \beta_2(\omega) \tag{11}$$

$$\partial\varphi/\partial x = 0 \quad \text{for} \quad r = \alpha_2(\omega),\ \omega \in \langle \omega_\mathrm{E}, \omega_\mathrm{D}\rangle \tag{12}$$

$$\partial\varphi/\partial y = 0 \quad \text{for} \quad r = \alpha_2(\omega),\ \omega \in \langle \omega_\mathrm{D}, \omega_0\rangle\,. \tag{13}$$

At this point, we introduce new coordinates ξ and η:

$$\xi = \omega \tag{14}$$

$$\eta = \begin{cases} r/\beta_1(\omega)\colon 0 \leqq r \leqq \beta_1(\omega) \\ \dfrac{r - \alpha_2(\omega)}{\beta_2(\omega) - \alpha_2(\omega)} + 1\colon \alpha_2(\omega) \leqq r \leqq \beta_2(\omega)\,, \end{cases} \tag{15}$$

where $\xi \in \langle 0, \omega_0\rangle$, $\eta \in \langle 0, 2\rangle$ (Fig. 4).

We can express the sought potential as a function of the new variables, $\psi(\xi, \eta)$, keeping in mind that $\psi(\xi(r, \omega), \eta(r, \omega)) = \varphi(r, \omega)$. Thus,

$$\frac{\partial^2\psi}{\partial\xi^2} F_1(\xi, \eta) + \frac{\partial^2\psi}{\partial\eta^2} F_2(\xi, \eta) + \frac{\partial\psi}{\partial\eta} F_3(\xi, \eta) + \frac{\partial^2\psi}{\partial\xi\,\partial\eta} F_4(\xi, \eta) + \frac{\partial\psi}{\partial\xi} F_5(\xi, \eta) = 0 . \tag{16}$$

Here we have introduced the following functions:

$$F_1 = 1/r^2 , \quad F_2 = \left(\frac{\partial\eta}{\partial r}\right)^2 + \frac{1}{r^2}\left(\frac{\partial\eta}{\partial\omega}\right)^2 \tag{17), (18}$$

$$F_3 = \frac{1}{r^2}\frac{\partial^2\eta}{\partial\omega^2} + \frac{\partial\eta}{\partial r}\left(\frac{2}{r} - \frac{1}{\varrho_M}\frac{\partial\varrho_M}{\partial r}\right) + \frac{1}{r^2}\frac{\partial\eta}{\partial\omega}\left(\frac{1}{\operatorname{tg}\omega} - \frac{1}{\varrho_M}\frac{\partial\varrho_M}{\partial\omega}\right) \tag{19}$$

$$F_4 = \frac{2}{r^2}\frac{\partial\eta}{\partial\omega}, \quad F_5 = \frac{1}{r^2 \operatorname{tg}\omega} - \frac{1}{\varrho_M r^2}\frac{\partial\varrho_M}{\partial\omega} . \tag{20), (21}$$

The variable r in Eqs (17)–(21) is expressed from (15) with regard to the corresponding region. Further we denote β_1 and β_2 the contour curves. From Eqs (14) and (15) we obtain

$$\frac{\partial\eta}{\partial r} = \begin{cases} 1/\beta_1 : 0 \leqq r \leqq \beta_1(\omega) \\ 1/(\beta_2 - \alpha_2) : \alpha_2(\omega) \leqq r \leqq \beta_2(\omega) \end{cases} \tag{22}$$

$$\frac{\partial\eta}{\partial\omega} = \begin{cases} -\eta\beta_1'/\beta_1 : 0 \leqq r \leqq \beta_1(\omega) \\ \dfrac{(\eta - 1)(\alpha_2' - \beta_2') - \alpha_2'}{\beta_2 - \alpha_2} : \alpha_2(\omega) \leqq r \leqq \beta_2(\omega) \end{cases} \tag{23}$$

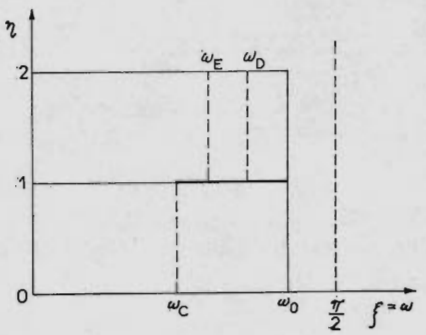

FIG. 4
Situation after transformation to a rectangle

$$\frac{\partial^2\eta}{\partial\omega^2} = \begin{cases} \eta(2\beta_1'^2 - \beta_1\beta_1'')/\beta_1^2 : 0 \leqq r \leqq \beta_1(\omega) \\ (\beta_2 - \alpha_2)^{-2}\{2[\alpha_2' + (\eta - 1)(\beta_2' - \alpha_2')](\beta_2' - \alpha_2') - \alpha_2''(\beta_2 - \alpha_2) - \\ - (\eta - 1)(\beta_2 - \alpha_2)(\beta_2'' - \alpha_2'')\} : \alpha_2(\omega) \leqq r \leqq \beta_2(\omega) . \end{cases} \tag{24}$$

The primes denote differentiation with respect to ξ. The boundary conditions for the solution of Eq. (*16*) are as follows:

$$\eta = 0 : \partial\psi/\partial\eta = 0 ; \quad \xi = 0 : \partial\psi/\partial\xi = 0 ; \tag{25), (26}$$

$$\frac{\partial\psi}{\partial\eta} K_1 + \frac{\partial\psi}{\partial\xi} K_2 = 0 \quad \text{for} \quad \begin{cases} \xi = \omega_0, \eta \in \langle 0, 2\rangle , \\ \xi \in \langle \omega_E, \omega_0\rangle, \eta = 1 . \end{cases} \tag{27}$$

On the boundary between regions *1* and *2*, the potential and its first derivatives must be continuous:

$$(\psi)_1 = (\psi)_2 , \quad (\text{grad}\,\psi)_1 = (\text{grad}\,\psi)_2 . \tag{28), (29}$$

The coefficients K_1, K_2 in (*27*) are given by the following equations:

$$K_1 = -\eta\beta_1'/\beta_1 : \xi = \omega_0, \eta \in \langle 0, 1\rangle ;$$

$$K_1 = \frac{(\eta - 1)(\alpha_2' - \beta_2') - \alpha_2'}{\beta_2 - \alpha_2} : \xi = \omega_0, \eta \in \langle 1, 2\rangle ;$$

$$K_1 = \frac{\cos\omega + \sin\omega(\alpha_2'/\alpha_2)}{\beta_2 - \alpha_2} : \xi \in \langle \omega_E, \omega_D\rangle, \eta = 1 ; \tag{30}$$

$$K_1 = \frac{\sin\omega - \cos\omega(\alpha_2'/\alpha_2)}{\beta_2 - \alpha_2} : \xi \in \omega_D, \langle\omega_0\rangle, \eta = 1 ;$$

$$K_2 = 1 : \xi = \omega_0, \eta \in \langle 0, 2\rangle ;$$

$$K_2 = -\sin\omega/\alpha_2 : \xi \in \langle \omega_E, \omega_D\rangle, \eta = 1 ; \tag{31}$$

$$K_2 = \cos\omega/\alpha_2 : \xi \in \langle \omega_D, \omega_0\rangle, \eta = 1 .$$

The potentials in the electrolyte at the anode or cathode surface are given by the following definitions:

$$E_A = \varphi_{m,A} - \varphi_{s,A} + \text{const.} , \quad E_K = \varphi_{m,K} + \varphi_{s,K} + \text{const.} \tag{32), (33}$$

Since the constants in these equations are related to the choice of the reference electrode, they can be set equal to zero. We can set also $\varphi_{m,K} = 0$, which means that $\varphi_{m,A}$ becomes equal to the terminal voltage, U, of the electrolyzer. Then

$$\psi_A = U - E_A(i_{n,A}), \quad \psi_K = -E_K(i_{n,K}), \qquad (34), (35)$$

where $U > 0$. The dependence of the electrode potentials E_A and E_K on the current density i_n is given by the Tafel equation in the form

$$\psi_A = U - E_{r,A} - a_A - b_A \ln i_{n,A}, \qquad (36)$$

$$\psi_K = -E_{r,K} + a_K + b_K \ln |i_{n,K}|. \qquad (37)$$

Close to the equilibrium potentials of the anode, $E_{r,A}$, and cathode, $E_{r,K}$, these equations are replaced by the equations of tangents to the polarization curves:

$$\psi_A = U - E_{r,A} - i_{n,A}/k_A, \quad \psi_K = -E_{r,K} + |i_{n,K}|/k_K. \qquad (38), (39)$$

Eqs (*38*) and (*39*) apply for small current densities defined as

$$i_{n,A} < \exp[(b_A - a_A)/b_A], \quad |i_{n,K}| < \exp[(b_K - a_K)/b_K], \qquad (40), (41)$$

whereas Eqs (*36*) and (*37*) apply for larger ones. Further we have

$$k_A = b_A^{-1} \exp[(b_A - a_A)/b_A], \quad k_K = b_K^{-1} \exp[(b_K - a_K)/b_K]. \qquad (42), (43)$$

The current density on the electrode surface is defined as

$$i_n = -\varrho_M^{-1}(\text{grad } \varphi)_n. \qquad (44)$$

For the anode, we have

$$(\text{grad } \varphi)_n = [1 + (\beta_2'/\beta_2)^2]^{-1/2} \left[\left(\frac{\partial \psi}{\partial \eta} \right)_{\beta_2} \left(\frac{\beta_2'^2}{\beta_2^2} + 1 \right) \frac{1}{\beta_2 - \alpha_2} - \left(\frac{\partial \psi}{\partial \xi} \right)_{\beta_2} \frac{\beta_2'}{\beta_2^2} \right]. \qquad (45)$$

For the cathode in region *1*

$$(\text{grad } \varphi)_{n,1} = [1 + (\beta_1'/\beta_1)^2]^{-1/2} \left[\left(\frac{\partial \psi}{\partial \eta} \right)_{\beta_1} \left(\frac{\beta_1'^2}{\beta_1^2} + 1 \right) - \left(\frac{\partial \psi}{\partial \xi} \right)_{\beta_1} \frac{\beta_1'}{\beta_1} \right] \frac{1}{\beta_1}, \qquad (46)$$

and in region *2*

$$(\text{grad } \varphi)_{n,2} = [1 + (\alpha_2'/\alpha_2)^2]^{-1/2} \left[\left(\frac{\partial \psi}{\partial \eta} \right)_{\alpha_2} \left(\frac{\alpha_2'^2}{\alpha_2^2} + 1 \right) \frac{1}{\beta_2 - \alpha_2} - \left(\frac{\partial \psi}{\partial \xi} \right)_{\alpha_2} \frac{\alpha_2'}{\alpha_2^2} \right]. \qquad (47)$$

In the point $\xi = \omega_C$, $\eta = 1$, which lies on the boundary of both regions, the current density is given as

$$|i_{n,K}| = (1/\varrho_M \sqrt{2}) [|(\text{grad } \varphi)_{n,1}| + |(\text{grad } \varphi)_{n,2}|] . \qquad (48)$$

Eqs (45)–(47) give the normal components if the gradients except for their sign which depends on the choice of the normal direction. Since the anodic current densities are taken positive and the cathodic ones negative, it is necessary to provide the mentioned normal components by the corresponding sign.

Calculation of the Specific Resistance of the Electrolyte

The following approximations were chosen for regions *1* and *2*, respectively, with regard to the primary current distribution and electrode shape:

$$\varrho_M = \text{const.}, \quad \partial\varrho_M/\partial r = 0 . \qquad (49), (50)$$

Further we neglect the heat formation during current passage through the electrodes and we assume that the temperature of the cathode surface is equal to that of the electrolyte in the given place. The anode has a constant temperature owing to its large mass. Since the temperature increment is of the order of 0·1 – 1 K, we do not consider the dependence of the electrode potential on the temperature. For the same reason, we consider the density S_E, specific heat $c_{p,E}$ and heat conductivity λ of the electrolyte approximately constant. We neglect the tension of water vapour in the bubbles and the transfer of heat into the bubbles during their passage through the system.

The specific resistance ϱ_M of the gas–electrolyte mixture is given as

$$\varrho_M = \varrho_E(1 + 1{\cdot}5\dot{V}_{G(\omega)}/\dot{V}_E) , \qquad (51)$$

and the volume rate of flow of the gas is

$$\dot{V}_{G(\omega)} = \dot{V}_{G,A(\omega)} + \dot{V}_{G,K(\omega)} . \qquad (52)$$

The rate of formation of the gas on the anode is given as

$$\dot{V}_{G,A} = \frac{2\pi R}{F P_{(\omega)}} \int_0^{\omega} T_{(\omega)} i_{n,A} \frac{P_{G,A}}{n_{G,A}} \beta_{2(\omega)} [\beta^2_{2(\omega)} + \beta'^2_{2(\omega)}]^{1/2} \sin \omega \, d\omega \qquad (53)$$

and the rate of gas formation on the cathode

$$\dot{V}_{G,K} = 0 : \omega \in \langle 0, \omega_C \rangle ,$$

$$\dot{V}_{G,K} = \frac{2\pi R}{FP_{(\omega)}} \int_{\omega_c}^{\omega} T_{(\omega)} i_{n,K} \frac{P_{G,K}}{n_{G,K}} \alpha_{2(\omega)} [\alpha_{2(\omega)}^2 + \alpha_{2(\omega)}'^2]^{1/2} \sin \omega \, d\omega : \omega \in \langle \omega_C, \omega_E \rangle ,$$

$$\dot{V}_{G,K} = \frac{2\pi R}{FP_{(\omega)}} \int_{\omega_c}^{\omega_E} T_{(\omega)} i_{n,K} \frac{P_{G,K}}{n_{G,K}} \alpha_{2(\omega)} [\alpha_{2(\omega)}^2 + \alpha_{2(\omega)}'^2]^{1/2} \sin \omega \, d\omega : \omega \in \langle \omega_E, \omega_0 \rangle . \quad (54)$$

The dependence of the specific resistance on the temperature can be expressed as[7]

$$\varrho_E = \varrho_E^0 / [1 + \delta(T - T_0)] . \quad (55)$$

The temperature in different points of the system can be calculated from the energetic balance

$$T = T_0 + (\dot{V}_E S_E c_{pE})^{-1} \int_0^{\omega} [\varrho_M \bar{i}_{A,K}^2 P_p (\nu^2 + \nu'^2)^{1/2} - 2\pi k_T (T - T_A) \beta_2 (\beta_2^2 + \beta_2'^2)^{1/2} . \\ . \sin \omega] \, d\omega . \quad (56)$$

Here we neglect the enthalpy change caused by electrode reactions; the mean current density $\bar{i}_{A,K}$ is defined as

$$\bar{i}_{A,K} = \tfrac{1}{2}(i_{n,A} + |i_{n,K}|) . \quad (57)$$

In the region outside the cathode, we set $i_{n,K} = 0$. The stream line $\nu(\omega)$ is defined as

$$\nu(\omega) = \tfrac{1}{2}(\alpha_{2(\omega)} + \beta_{2(\omega)}) . \quad (58)$$

The coefficient of heat transfer, k_T, is calculated from the definition of the Nusselt criterion

$$\mathrm{Nu} = 4 k_T P_p / \lambda O \quad (59)$$

and this criterion is calculated as

$$\mathrm{Nu} = 0{\cdot}023 \, \mathrm{Re}^{0.8} \, \mathrm{Pr}^{0.4} , \quad (60)$$

with

$$\mathrm{Re} = 4 \dot{V}_E S_E / O \mu , \quad \mathrm{Pr} = c_p \mu / \lambda . \quad (61), (62)$$

The transfer of heat is calculated from equations valid for a fully developed turbulent profile, so that in our case, where the cross section along the stream line changes, our values are subject to a certain error. We use the following approximation for the dependence of the viscosity on the temperature[8]

$$\varrho_E/\mu = \text{const.} \tag{63}$$

The pressures in different points of the system are given as

$$P(\omega) = P^0 - \Delta P_z - \int_0^\omega \frac{0{\cdot}3164 S_E(1 - f_{(\omega)})O}{4\,\mathrm{Re}_M^{1/4} P_p} \left(\frac{\dot{V}_E}{P_p}\right)^2 \frac{(v^2 + v'^2)^{1/2}}{(1 - f_{(\omega)})^2}\,\mathrm{d}\omega\,, \tag{64}$$

where[9]

$$\mathrm{Re}_M = \mathrm{Re}(1 - f_{(\omega)})^{2.5}\,, \quad f_{(\omega)} = \dot{V}_G/(\dot{V}_E + \dot{V}_G)\,. \tag{65), (66}$$

The pressure loss in the cathode is calculated as

$$\Delta P_z = \frac{S_E L}{4 r_V} \left(\frac{\dot{V}_E}{\pi r_V^2}\right)^2 f_T\,. \tag{67}$$

The cross-sectional area of flow in Eq. (64) is defined as

$$\begin{aligned} P_p &= \pi C[2(\beta_2 \cos\omega_c - B)\,\omega/\omega_c + C(1 - \omega/\omega_c)]\colon \omega \in \langle 0, \omega_c\rangle\,, \\ P_p &= 2\pi\alpha_2 \sin\omega(\beta_2 \cos\omega - B)\colon \omega \in \langle \omega_c, \omega_E\rangle\,, \\ P_p &= \pi(\beta_2^2 - \alpha_2^2)\sin\omega\colon \omega > \omega_E \end{aligned} \tag{68}$$

and the wetted circumference O

$$\begin{aligned} O &= 2\pi(C + (\omega/\omega_c)\,\beta_2 \sin\omega_c)\colon \omega \in \langle 0, \omega_c\rangle\,, \\ O &= 2\pi(\beta_2 + \alpha_2)\sin\omega\colon \omega > \omega_c\,. \end{aligned} \tag{69}$$

Since the temperature and pressure cannot be expressed explicitly from the preceding equations, we proceed by iterations calculating alternatively the temperature and the pressure; we use the relations

$$P_{(\omega)}^{S+1} = C_1 P_{(\omega)}^N + (1 - C_1)\,P_{(\omega)}^S\,, \tag{70}$$

$$T_{(\omega)}^{S+1} = C_2 T_{(\omega)}^N + (1 - C_2)\,T_{(\omega)}^S\,, \tag{71}$$

where $C_1, C_2 \in \langle 0{\cdot}1, 0{\cdot}3\rangle$.

Calculation of Boundary Conditions and Shape of Anode

It is necessary to ensure the fulfilment of the boundary conditions (25)–(29), (34) and (35). This is achieved as follows. The derivatives in (25)–(27) and (29) are ex-

pressed by difference formulas (see below); symmetrical or asymmetrical formulas are used according to the position of the grid point in the network. The obtained difference equations enable us to express the potential in a given point by means of the potentials in neighbouring points. We take an aliquote part from the calculated value ψ_N of the potential:

$$\psi^{S+1} = C_3\psi^N + (1 - C_3)\,\psi^S\,, \tag{72}$$

where $C_3 \in \langle 0{\cdot}05, 1\rangle$. We proceed by this iteration method until the corresponding boundary conditions are fulfilled in the whole line. Thus, the potentials on the boundaries are corrected after every 5 to 20 iterations within the field.

The potentials in Eqs (*34*) and (*35*) are calculated after every iteration within the field. An aliquote part is taken according to Eq. (*72*) with $C_3 \approx 0{\cdot}005$ from newly calculated values. To ensure convergence within the field of potentials, the last correction is performed only when the error within the field drops below a predetermined value.

To check the accuracy of the calculation, we calculate the total currents on the anode and cathode from the equations

$$I_A = 2\pi \int_0^{\omega_0} i_{n,A}\beta_2(\omega)\left[\beta_2^2(\omega) + \beta_2'^2(\omega)\right]^{1/2} \sin\omega\,\mathrm{d}\omega \tag{73}$$

$$I_K = 2\pi \int_{\omega_c}^{\omega_0} i_{n,K}\beta_1(\omega)\left[\beta_1^2(\omega) + \beta_1'^2(\omega)\right]^{1/2} \sin\omega\,\mathrm{d}\omega + \\ + \int_{\omega_c}^{\omega_E} i_{n,K}\alpha_2(\omega)\left[\alpha_2^2(\omega) + \alpha_2'^2(\omega)\right]^{1/2} \sin\omega\,\mathrm{d}\omega\Big]\,. \tag{74}$$

After the required accuracy of the potentials (both in the field and on the border), temperatures, and pressures is attained, the change of the anode shape is calculated. We assume that the current densities on the electrode surface do not change during a small time interval $\Delta\tau$, so that the rate of change of the anode surface in the normal direction, Δn (m/s), can be calculated as

$$\Delta n = M_A i_{n,A} P_I / nFS_A\,, \tag{75}$$

where P_I is the current yield of the anodic dissolution of the metal

$$\mathrm{Me} = \mathrm{Me}^{n+} + \mathrm{ne}^-\,. \tag{76}$$

The parametric equations describing the shape of the anode in coordinates x, y

as a function of the polar angle

$$x = \beta_2(\omega)\cos\omega\,, \quad y = \beta_2(\omega)\sin\omega \qquad (77), (78)$$

serve to calculate the changes of the coordinates of the grid points (x_i, y_i) on the anode surface with time; the shift of the cathode at a velocity v_x parallel to the x axis is taken into account:

$$\Delta x = (\Delta n(1 + s^2)^{-1/2} - v_x)\,\Delta\tau\,, \qquad (79)$$

$$\Delta y = \Delta n s(1 + s^2)^{-1/2}\,\Delta\tau\,. \qquad (80)$$

The variable s is defined as

$$s = (\beta_2 \sin\omega - \beta_2' \cos\omega)/(\beta_2' \sin\omega + \beta_2 \cos\omega)\,. \qquad (81)$$

Thus, we obtain a table of the coordinates (x_i^N, y_i^N) of points lying on the new anode surface and calculated as

$$x_i^N = x_i + \Delta x_i\,, \quad y_i^N = y_i + \Delta y_i\,. \qquad (82), (83)$$

The new cartesian coordinates (x_i^N, y_i^N) are converted to polar coordinates $(\beta_{2i}^N, \omega_i^N)$ by means of Eqs (77) and (78), whence the polar coordinates of points on the new surface corresponding to predetermined grid points are calculated by quadratic interpolation.

The values of $\Delta\tau$ must be relatively small to make the changes in the electrode shape also small, thus suppressing the computational error. The described method of calculation of new values of $\beta_2(\omega)$ corresponds to the Euler's method of integration.

If we choose a sufficiently large velocity of the electrode shift v_x, we can simulate the contact of the electrodes similarly to a practical case.

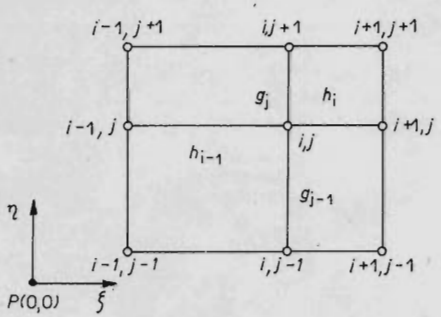

FIG. 5
Grid points and their indexing

Approximation of Derivatives by Difference Formulas

We shall consider a two-dimensional nonequidistant network (Fig. 5), in which the derivatives are approximated by difference formulas with an error of $O(h^2)$ or $O(g^2)$:

$$\left(\frac{\partial f}{\partial \xi}\right)_{i,j} = \frac{f_{i+1}h_{i-1}^2 + f_i(h_i^2 - h_{i-1}^2) - f_{i-1}h_i^2}{h_i h_{i-1}(h_i + h_{i-1})} \tag{84}$$

$$\left(\frac{\partial^2 f}{\partial \xi^2}\right)_{i,j} = \frac{f_{i+1}h_{i-1} - f_i(h_i + h_{i-1}) + f_{i-1}h_i}{0{\cdot}5h_i h_{i-1}(h_i + h_{i-1})} \tag{85}$$

$$\left(\frac{\partial^2 f}{\partial \xi\, \partial \eta}\right)_{i,j} =$$

$$= \frac{h_i}{h_{i-1}(h_i + h_{i-1})}\left[\frac{f_{i-1,j-1}g_j}{g_{j-1}(g_j + g_{j-1})} - f_{i-1,j}\frac{g_j - g_{j-1}}{g_j g_{j-1}} - \frac{f_{i-1,j+1}g_{j-1}}{g_j(g_j + g_{j-1})}\right] +$$

$$+ \frac{h_i - h_{i-1}}{h_i h_{i-1}}\left[-\frac{f_{i,j-1}g_j}{g_{j-1}(g_j + g_{j-1})} + f_{i,j}\frac{g_j - g_{j-1}}{g_j g_{j-1}} + \frac{f_{i,j+1}g_{j-1}}{g_j(g_j + g_{j-1})}\right] +$$

$$+ \frac{h_{i-1}}{h_i(h_i + h_{i-1})}\left[-\frac{f_{i+1,j-1}g_j}{g_{j-1}(g_j + g_{j-1})} + f_{i+1,j}\frac{g_j - g_{j-1}}{g_j g_{j-1}} + \frac{f_{i+1,j+1}g_{j-1}}{g_j(g_{j-1} + g_j)}\right]. \tag{86}$$

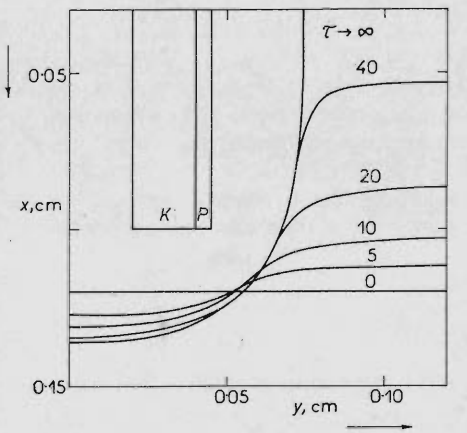

FIG. 6

Time course of machining taking into account the influence of polarization, heat and bubbles. Time τ is given in seconds. Thickness of insulating layer 50 μm

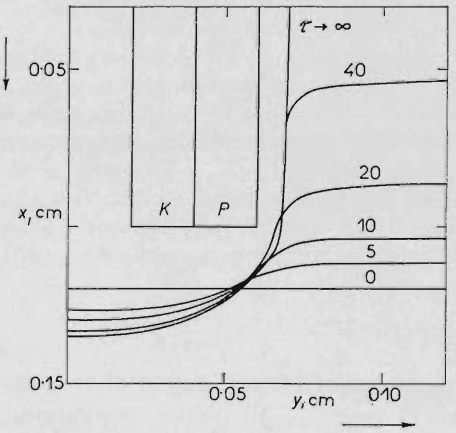

FIG. 7

Time course of machining taking into account the influence of polarization, heat, and bubbles. Time τ is given in seconds. Thickness of insulating layer 200 μm

Asymmetrical formulas are used for the border of the network. If the values for subscripts $i + 1$ and $i + 2$ are known, the following equation is preferred:

$$\left(\frac{\partial f}{\partial \xi}\right)_{i,j} = \frac{(f_{i+1} - f_i)(h_i + h_{i+1})^2 - (f_{i+2} - f_i) h_i^2}{h_i h_{i+1}(h_i + h_{i+1})} . \tag{87}$$

If the values in points with subscripts $i - 1$ and $i - 2$ are known, then

$$\left(\frac{\partial f}{\partial \xi}\right)_{i,j} = \frac{(f_{i-2} - f_i) h_{i-1}^2 - (f_{i-1} - f_i)(h_{i-2} + h_{i-1})^2}{h_{i-1} h_{i-2}(h_{i-1} + h_{i-2})} . \tag{88}$$

Eqs (*87*) and (*88*) are needed in calculating the potential gradients at the electrodes and in approximating the boundary conditions.

The iterative calculation of potentials in given points is carried out by the superrelaxation method[5], *i.e.*, according to the relations

$$\psi_{i,j}^{S+1} = \psi_{i,j}^{S} + r_{i,j} R_{i,j}^{S} z . \tag{89}$$

The superscripts S, $S + 1$ denote the order number of the corresponding iteration. The values of the residues $R_{i,j}^{S}$ are calculated by substituting the S-th values of the potentials into the left side of Eq. (*16*), in which the derivatives are expressed from the approximate Eqs (*84*)—(*86*). The convergence of the potentials ψ^S was achieved by the following choice of the relaxation factor $r_{i,j}$:

$$r_{i,j}^{-1} = \frac{2}{h^2} |F_1(\xi, \eta)| + \frac{2}{g^2} |F_2(\xi, \eta)| + \frac{1}{g} |F_3(\xi, \eta)| + \frac{1}{gh} |F_4(\xi, \eta)| + \frac{1}{h} |F_5(\xi, \eta)| , \tag{90}$$

where h denotes the least value of h_i and h_{i-1} and g the least value of g_i and g_{i-1}. By this choice of the relaxation factor, the row vector of the matrix of coefficients of the solved system of differential equations is minimized and thus the convergence of the sequence of iterations ψ^S is ensured.

The multiplicative factor z in Eq. (*89*) is an empirically found constant which ensures and accelerates the convergence. The maximum value of z, for which the system at the given moment still converges is used; in our case $z \in \langle 2; 2{\cdot}6 \rangle$.

RESULTS

The results of the calculation of the course of electrochemical drilling (cf. Formulation of the problem) are presented graphically in Figs 6 and 7. A network of 19 × 16 points was used.

The input data were the following:

inner diameter of cathode 0·4 mm (r_V);
outer diameter of cathode 0·8 mm;
thickness of insulation on the outer cathode surface 0·05 mm;

initial anode-cathode distance 0·2 mm;
terminal voltage after subtracting equilibrium potentials $U - E_{i,A} + E_{r,K} = 20{\cdot}0$ V;
constants of Tafel equation $a_A = -0{\cdot}1526$ V, $b_A = 0{\cdot}06$ V, $a_K = 0{\cdot}0526$ V; $b_K = 0{\cdot}06$ V;
specific resistance of electrolyte at the inlet $\varrho_E^0 = 0{\cdot}0555\ \Omega$m;
density of electrolyte $S_E = 1\ 329$ kg/m^3;
heat conductivity of electrolyte $\lambda = 0{\cdot}55$ W/m K;
specific heat of electrolyte $c_{p,E} = 3\ 400$ J/kg K;
dynamic viscosity of electrolyte $\mu = 1{\cdot}60 \cdot 10^{-3}$ kg/m s;
constant in Eq. (*55*) $\delta = 0{\cdot}0179$ K^{-1};
volume rate of flow of electrolyte $\dot{V}_E = 2{\cdot}8 \cdot 10^{-6}$ m^3/s;
coefficient of friction $f_T = 0{\cdot}09$;
length of cathode $L = 40$ mm;
electrolyte temperature at the inlet 20°C;
anode temperature 20°C;
pressure of electrolyte 1 MPa;
current yield for dissolution of anode metal $P_I = 0{\cdot}65$;
current yields for gas formation $P_{G,A} = 0{\cdot}35$, $P_{G,K} = 1{\cdot}00$;
rate of shift of cathode $v_x = 1{\cdot}667 \cdot 10^{-5}$ m/s.

TABLE I

Profile of anode and primary current distribution on electrodes in stationary state

ξ	$\beta_2 \cdot 10^2$ m	$i_{\beta_2} \cdot 10^{-4}$ A/m^2	$\lvert i_{\alpha_2} \rvert \cdot 10^{-4}$ A/m^2	$\lvert i_{\beta_1} \rvert \cdot 10^{-4}$ A/m^2
0·000	0·1368	69·9	—	—
0·047	0·1369	69·9	—	—
0·090	0·1369	69·7	—	—
0·130	0·1370	69·4	—	—
0·165	0·1370	68·9	—	—
0·197	0·1370	68·3	176·5	176·5
0·234	0·1369	67·3	153·4	0·0
0·271	0·1366	65·8	160·1	0·0
0·307	0·1362	63·9	184·2	0·0
0·344	0·1355	61·2	251·4	0·0
0·381	0·1347	57·8	440·4	0·0
0·427	0·1331	51·4	—	0·0
0·487	0·1299	40·5	—	0·0
0·564	0·1242	27·9	—	0·0
0·663	0·1151	15·8	—	0·0
0·788	0·1037	6·5	—	0·0
0·949	0·0920	1·9	—	0·0
1·156	0·0817	0·6	—	0·0
1·419	0·0757	0·0	—	0·0

We consider an iron anode which oxidises to form Fe^{2+} ions. The electrolyte contains about 200 g NaCl in 1 dm^3. We choose $\Delta\tau = 1$ s. The stationary profile of the anode was formed after 60 s of electrolysis (with an error smaller than 1% in all points).

The calculations lead to the values of current densities on the anode and cathode surfaces (Tables I and II). The total currents on the anode and cathode differed by less than 20% in both versions of the calculations ($I_A = 1{\cdot}25$ A and $I_K = 1{\cdot}06$ A in the case of primary current distribution, $I_A = 1{\cdot}20$ A and $I_K = 0{\cdot}99$ A when the influence of polarization, Joule heat, and gas bubbles was taken into account). We can safely assume that the error in the calculated current density and hence in the anode shape is smaller, since with respect to the shape of the anode the error in the total current is given prevailingly by the points that are most distant from the axis of symmetry and in which almost no dissolution proceeds.

It follows from the comparison of the results of both versions that polarization, heat, and bubbles have a very limited influence on the shape of the workpiece. The corresponding temperature increment is only 1·5 K, the volume fraction of bubbles

TABLE II

Profile of anode and distribution of current density, pressure and temperature in stationary state

ξ	$\beta_2 \cdot 10^2$ m	$i_{\beta_2} \cdot 10^{-4}$ A/m^2	$\lvert i_{\alpha_2}\rvert \cdot 10^{-4}$ A/m^2	$\lvert i_{\beta_1}\rvert \cdot 10^{-4}$ A/m^2	P MPa	T °C
0·000	0·1350	69·9	—	—	0·9988	20·000
0·047	0·1351	69·9	—	—	0·9966	20·010
0·090	0·1352	69·7	—	—	0·9957	20·016
0·130	0·1352	69·4	—	—	0·9952	20·022
0·165	0·1353	69·0	—	—	0·9949	20·030
0·197	0·1353	68·4	155·2	155·2	0·9947	20·076
0·234	0·1352	67·4	145·6	0·0	0·9945	20·176
0·271	0·1350	66·0	152·4	0·0	0·9943	20·288
0·307	0·1347	64·1	175·2	0·0	0·9941	20·427
0·344	0·1341	61·4	248·1	0·0	0·9939	20·633
0·381	0·1332	58·0	424·3	0·0	0·9937	21·093
0·427	0·1317	51·2	—	0·0	0·9935	21·525
0·487	0·1284	39·6	—	0·0	0·9933	21·545
0·564	0·1225	26·4	—	0·0	0·9932	21·565
0·663	0·1132	14·2	—	0·0	0·9930	21·577
0·788	0·1014	5·5	—	0·0	0·9928	21·583
0·949	0·0894	1·8	—	0·0	0·9927	21·586
1·156	0·0793	0·6	—	0·0	0·9925	21·588
1·419	0·0734	0·0	—	0·0	0·9923	21·588

in the outflowing electrolyte being smaller than 1%. To judge the influence of the thickness of the insulating layer on the shape of the orifice of the drilled hole, calculations were carried out for 50 μm and 200 μm thick insulations (Figs 6 and 7). A favourable influence of the thicker insulation on the shape of the orifice in a horizontal plane is seen from the figures.

Remarks to the Simulation Program

Calculations were carried out on an ICL 4—72 type computer and the network had 304 points. The calculation of the potential distribution at the beginning is most time-consuming (about 30 min). During changes of the anode shape, the distribution of potential in space does not change appreciably; one change of the anode shape requires only 10—20 s of the computer time. Taking into account the polarization, heat, and bubbles increases the computer time approximately by 5—15%. The results show that the approximation without polarization is sufficient.

LIST OF SYMBOLS

a, b	constants of the Tafel equation (V)
A, B, C, D, E	dimensions of the system (m)
C_{pE}	specific heat of electrolyte (J/kg K)
C_i	constants
E	potential (V)
f_T	coefficient of friction
F	Faraday's constant (C/mol)
F_i	auxiliary functions ($i = 1$—5), Eqs (*17*)—(*21*)
g_i	distance between grid points along η coordinate
h_i	distance between grid points along ξ coordinate
i	current density (A/m^2)
I	total current between electrodes (A)
k_A, k_K	constants, Eqs (*42*) and (*43*)
k_T	coefficient of heat transfer (W/m^2 K)
K_1, K_2	coefficients, Eqs (*30*) and (*31*)
L	length of cathode (m)
M_A	molar mass of anode metal (kg/mol)
n	number of electrons exchanged in anodic dissolution
n_G	number of electrons exchanged in gas forming reaction
Δn	rate of shift of anode in normal direction (m/s)
Nu	Nusselt criterion
O	wetted perimenter (m)
P_G	current yield in gas evolution
P_I	current yield in dissolution of anode metal
ΔP_z	pressure loss in cathode (Pa)
P_p	cross sectional area of flow (m^2)
Pr	Prandtl criterion
r	radius (m)
r_V	inner radius of cathode (m)
$r_{i,j}$	relaxation factor
R	universal gas constant (J/mol K)

$R_{i,j}$	residuum
Re	Reynolds criterion
Re_M	criterion defined by Eq. (*65*)
s	slope, Eq. (*81*)
S_E	density of electrolyte (kg/m^3)
T	absolute temperature (K)
U	terminal voltage of electrolyser (V)
v_x	rate of shift of tool (m/s)
$\dot{V}$	volume rate of flow (m^3/s)
x, y	cartesian coordinates in cross section of the system (m)
x', y', z'	cartesian coordinates in space (m)
z	empirical constant
α, β	curves expressing the limits of the system
γ	curve expressing the shape of anode
δ	constant in Eq. (*55*)
η	transformed radius r
λ	heat conductivity of electrolyte (W/m K)
μ	dynamic viscosity of electrolyte (kg/m s)
ν	stream line
ξ	transformed coordinate ω
ϱ	specific resistance (Ω m)
τ	time (s)
υ	spherical coordinate
φ	potential in coordinates r, ω (V)
ψ	potential in coordinates ξ, η (V)
ω	spherical (polar) coordinate

Subscripts or superscripts:

A anode, E electrolyte, G gas phase, K cathode, m metal, M gas-electrolyte mixture, n normal component, N new value in iteration, r equilibrium value, s interface (on the electrolyte side), S order number of iteration, 0 value in point (0, 0), *1*, *2* region of calculation.

REFERENCES

1. McGeough J. A.: *Principles of Electrochemical Machining*, p. 218. Chapman and Hall, London 1974.
2. Wilson J. F.: *Practice and Theory of Electrochemical Machining*, p. 136. Willey-Interscience, New York 1971.
3. De Barr A. E., Oliver D. A.: *Electrochemical Machining*, p. 158. McDonald, London 1968.
4. Ref. 1, p. 227.
5. Novák P., Roušar I., Kimla A., Cezner V., Mejta V.: This Journal *45*, 1867 (1980).
6. Novák P., Kimla A., Roušar I., Cezner V., Mejta V.: This Journal *45*, 1456 (1980).
7. Kotora J.: *Thesis*. Prague Institute of Chemical Technology, Prague 1979.
8. Robinson R. A., Stokes R. H.: *Electrolyte Solutions* (in Russian), p. 64. Izd. inostr. literatury, Moscow 1963.
9. Zuber N.: Chem. Eng. Sci. *19*, 897 (1964).

Translated by K. Micka.